Atmospheric Chemistry Signatures of an Equatorially-Symmetric Matsuno-Gill Circulation Pattern

Catherine Wilka[1], Susan Solomon[1], Timothy W Cronin[1], Doug Kinnison[2], Rolando Garcia[2]

[1] Department of Earth, Atmospheric, and Planetary Sciences, Massachusetts Institute of Technology, Cambridge, MA, USA.

[2]Atmospheric Chemistry Observations and Modeling Laboratory, National Center for Atmospheric Research, Boulder, CO, USA

Corresponding author: Catherine Wilka (cwilka@mit.edu)

Abstract

Matsuno-Gill circulations have been widely studied in tropical meteorology, but their impact on stratospheric chemistry has seldom been explicitly evaluated. This study demonstrates that, in a model nudged to reanalysis, anticyclonic Rossby wave gyres that form near the tropopause due to equatorially-symmetric heating in the troposphere provide a dynamical mechanism to influence tropical and subtropical atmospheric chemistry during near-equinox months. The anticyclonic flow entrains extratropical air from higher latitudes into the deep tropics of both hemispheres and induces cooling in the already cold upper-troposphere/lower-stratosphere (UTLS) region. Both of these aspects of the circulation allow heterogeneous chlorine activation on sulfuric acid aerosols to proceed rapidly, primarily via the HCl + $ClONO_2$ reaction. Precipitation rates and heating rates from reanalysis are shown to be consistent with these heating and circulation response patterns in the months of interest. This study analyzes specified dynamics simulations from the Whole Atmosphere Community Climate Model (SD-WACCM) with and without tropical heterogeneous chemistry to demonstrate that these circulations influence substantially the distributions of, for example, NO_2 and ClO in the UTLS tropics and subtropics of both hemispheres. This provides a previously unrecognized dynamical influence on the spatial structures of atmospheric composition changes in the UTLS during near-equinox months.

1 Introduction

Matsuno (1966) studied the equatorial waves produced in response to equatorial heating in the context of a linearized, beta-plane model, successfully identifying the equatorially trapped Kelvin wave and the off-equator Rossby wave gyre responses. Gill (1980) imposed both symmetric and asymmetric heating across the equator and calculated the response of the tropical atmosphere to these idealized perturbations using linear theory. Both papers show variants of a “bulls-eye” pattern in pressure perturbations (Matsuno Figure 9 and Gill Figure 1b), which are now seen as indicative of the Matsuno-Gill response. While the real atmosphere is more complicated than these simplified models, and the assumptions of steady heating and time-invariance are never perfectly valid, the basic patterns have been identified in multiple dynamical studies (Jin and Hoskins 1995, Adames and Wallace 2017, Rodwell and Hoskins 2001, among others). The wind response takes the form of two Rossby cyclones in the lower troposphere and is overlain by anticyclones in the UTLS, which are located to the northwest and southwest of the heating maximum, as well as an equatorially trapped Kelvin wave to the east over the Pacific, with easterly flow in the lower troposphere and westerly flow aloft. These zonal asymmetries in the Matsuno-Gill pattern decay upward into the stratosphere, with ascent and anomalously cold air in the lower stratosphere overlying regions of deep convection and greatest tropopause heights. The dynamics of this pattern have been widely studied in the decades since its description; here we examine some of its impacts on UTLS chemistry, which result from the combination of winds and temperature anomalies.

55 The importance of heterogenous chlorine activation reactions to ozone depleting
56 chemistry has been well established for decades (Solomon et al. 1986, Solomon 1999
57 and references therein) and is known to be the key driver of the so-called “ozone hole.”
58 Heterogeneous reactions on stratospheric aerosols convert chlorine from the reservoir
59 species HCl and $ClONO_2$ to active forms that can destroy ozone in catalytic cycles. Of
60 particular importance are the $HCl + ClONO_2 \rightarrow Cl_2 + HNO_3$, $H_2O + ClONO_2 \rightarrow HOCl +$
61 HNO_3, and $HCl + HOCl \rightarrow H_2O + Cl_2$ reactions. Multiple factors influence the rates of
62 these reactions, including temperature, water vapor levels, chlorine precursor levels,
63 and aerosol surface area. The $HCl + ClONO_2$ reaction, which is in many regions the
64 dominant source of activation, has an extremely strong inverse temperature
65 dependence, with reaction efficiencies that decrease by six orders of magnitude
66 between 190 K and 205 K. This dependence is due to multiple factors, but below 200 K
67 is dominated by the increasing solubility of HCl with decreasing temperature (Shi et al.
68 2001). The importance of these reactions has been extensively studied in the Arctic and
69 Antarctic for decades, and in recent years there has been an increased focus on the
70 potential for this chemistry to proceed outside the polar regions, specifically on liquid
71 sulfuric acid aerosols that are ubiquitous in the lower stratosphere (Anderson et al.
72 2017, Robrecht et al. 2019).
73
74 Solomon et al. (2016) showed that the strong anticyclone of the East Asian
75 Summer Monsoon (EASM) is capable of entraining chlorine (in the form of HCl) from
76 higher latitudes. This chlorine enters the upper troposphere/lower stratosphere (UTLS)
77 region above the EASM anticyclone, where temperatures are anomalously cold due to

78 the response to convective heating (Highwood and Hoskins 1998). This combination of
79 increased chlorine mixing ratios and cold temperatures drives chlorine activation. This
80 work motivates us to consider additional conditions for moving chlorine into cold regions
81 in the tropics that are difficult to describe in a zonally-averaged framework, such as has
82 often been used in the past to study meridional gradients in stratospheric chemical
83 species. An overall goal is to contribute to a growing body of research that considers the
84 effect of eddies and other longitudinally asymmetric features on stratospheric
85 composition and chemistry. Identifying such features would provide an improved
86 understanding of coupling between chemistry and transport, and a potential target for
87 future observational campaigns in the tropical UTLS.
88
89 Matsuno-Gill tropical circulation patterns have seldom been studied in connection
90 with stratospheric chemistry until recently. Solomon et al. (2016) was one of the first
91 studies to investigate the response of stratospheric chlorine to equatorially-asymmetric
92 heating of this type, and this work extends that by looking at the equatorially-symmetric
93 case, which is more typically found in near-equinox months. Compared to the EASM
94 anticyclone, the equatorially-symmetric Matsuno-Gill anticyclones are somewhat weaker
95 and situated deeper in the tropics, so they advect less chlorine from higher latitudes.
96 However, since the tropopause temperatures in the deep tropics are lower on average
97 than those at the latitude of the EASM anticyclone, the negative temperature
98 perturbations from this type of Matsuno-Gill circulation nonetheless drive very swift
99 chlorine activation. As explored below, this circulation pattern provides a pathway for

chlorine activation in the deep tropics in months where activation has not previously been considered.

2 Methods

2.1 Rainfall Data

We use NOAA's Global Precipitation Climatology Project (GPCP) version 2.3 to investigate precipitation patterns, which are a good observable proxy for heating due to latent heat release. The GPCP combines observations from rain gauge stations and soundings with satellite precipitation data to produce a 2.5°x2.5° resolution global product that covers land and ocean at monthly resolution from 1979 to present day (Adler et al. 2003).

2.2 Model

We use NCAR's Community Earth System Model with a "specified dynamics" (SD) version of the Whole Atmosphere Community Climate Model, version 4 as the atmospheric component. This model configuration is formally denoted CESM(SD-WACCM4), but throughout this paper we refer to it simply as SD-WACCM. Below 50 km, SD-WACCM is nudged to externally specified temperature, zonal and meridional wind, and surface pressure fields from the Modern Era Retrospective Analysis for Research and Applications (MERRA), with a relaxation time of 50 hours. MERRA is a global atmospheric reanalysis beginning in 1979 and continuing through 2016 that is produced and maintained by NASA (Rienecker et al. 2011). To investigate heating

123 rates, we present monthly means derived from the daily mean output files for each
124 pressure level of interest for the diabatic heating.
125
126 WACCM is a high-top model with detailed gas-phase and heterogeneous
127 chemistry schemes that include the O_x, NO_x, HO_x, ClO_x, and BrO_x reaction families. The
128 chemistry is fully interactive, with a timestep of 30 minutes, and the model has been
129 extensively evaluated for use in stratospheric studies (Marsh et al. 2013, Mills et al.
130 2017, Froidevaux et al. 2019). About 5 pptv of very short-lived substances (VSLS) are
131 included in the total bromine loading, but chlorine from VSLS is not included.
132 Heterogeneous reactions on cirrus ice particles are not included. SD-WACCM has 1.9 x
133 2.5° (latitude-longitude) horizontal resolution, with 88 pressure levels from the surface
134 up to 140 km. Stratospheric sulfate aerosols are modeled as three lognormal modes
135 and include the effect of nucleation, condensation, coagulation, and sedimentation in a
136 microphysics scheme described in detail in Mills et al 2016. The background sulfur
137 loading from volcanic eruptions is taken from a database developed by Neely and
138 Schmidt 2016 that specifies plume injection height and the amount of sulfur injected.
139
140 We consider two different runs of SD-WACCM over four years from 2009 to
141 2012. In the first run, labeled Chem-Dyn-Vol, the effects of chemistry, dynamics, and
142 volcanic eruptions are all included. This run is the standard and, in SD-WACCM,
143 represents the best attempt to simulate the real world for those years. Note, however,
144 that the chemical scheme in Chem-Dyn-Vol does not include water ice chemistry; the
145 implications of this are discussed below, in Section 4. The second run, labeled

NoHet40NS, turns off all heterogeneous reactions involving chlorine and bromine between 40°N and 40°S but permits heterogeneous reactions not involving these species. Temperatures at mid-latitudes are too warm to drive the heterogeneous chemistry of interest here. Comparing these two runs allows us to isolate the signature of in-situ tropical heterogeneous chlorine and bromine chemistry as distinct from polar regions. We examine monthly-mean output for this study, and discuss the potential influence of more transient behavior in Section 4.

We focus on "near equinox" months for this analysis, so the influence from summer monsoonal patterns in either hemisphere should be limited. As an example, we present results below for November, 2009 (a month without a major stratospheric-impacting volcanic eruption) but note that equatorially-symmetric Matsuno-Gill patterns are identified in other months as well. The impacts of these Matsuno-Gill patterns are manifested in chemical responses in low latitudes of both hemispheres, whereas responses to heating displaced from the Equator, such as the EASM, are confined to the warm season hemisphere of active monsoon rainfall. We find similar results in several other shoulder months in the four-year time series we looked at, including April 2009 and 2011, November 2011, and March 2012. We expect that in a longer time series there would be many more examples.

3 Results

168 Figure 1a shows the mean precipitation rate for November 2009 from 40°N to
169 40°S from the GPCP. The highest rates occur over the equatorial Indian Ocean and
170 over the western Pacific Ocean between 15°N to 15°S. These areas are therefore
171 regions of strong latent heat release, and are a better marker of tropical diabatic heating
172 locations than sea surface temperature would be. We examine the diabatic heating
173 rates at multiple levels in MERRA, which provides the meteorological fields for SD-
174 WACCM as described above, and find that the heating tendency (K/day) due to physics
175 is at a maximum near 400 mb, as shown in Figure 1b for November 2009. Although the
176 real-world response is more varied, this resembles the vertical profile of the heating
177 prescribed in the Gill model. The maximum in the deep tropics and the north-and-
178 southward extending lobes track the observed precipitation patterns closely, as we
179 would expect given the close linkage between diabatic heating rates and latent heat
180 release. While the heating itself extends further into the Southern Hemisphere than the
181 Northern Hemisphere, anomalies are clearly visible in both hemispheres. These heating
182 rates decay higher in the troposphere, and at and above the tropopause there is little
183 remnant in the diabatic heating signal. By 100 mbar (Figure S1), the signal has
184 vanished.
185
186 Figure 2a shows the vector winds and temperatures in SD-WACCM on the 85
187 mb level for November 2009. The wind response to the heating pattern consists of
188 cyclonic behavior in the lower troposphere and mirrored anticyclonic behavior in the
189 lower stratosphere. Anticyclones can be seen in Figure 2a on the poleward flanks of the
190 heating pattern, specifically east of Taiwan and off the northeast coast of Australia. The

eastward-propagating Kelvin wave characteristic of the Matsuno-Gill is manifested by the pattern of eastward winds visible in the equatorial Pacific east of the dateline, toward the eastern part of the 192 K temperature contour. The anticyclones provide a mechanism, analogous to the anticyclone of the EASM, to entrain chlorine in reservoir form from higher latitudes. We see this when we examine SD-WACCM's November 2009 HCl distribution at 85 mbar in Figure 2b. Higher volume mixing ratios track the anticyclone near 160°E in the Northern Hemisphere and 140°E in the Southern Hemisphere, enhancing HCl by 50-100 pptv above what is seen in the rest of the Pacific at those latitudes. The other main form of reservoir chlorine, $ClONO_2$, is also enhanced by this effect, as can be seen in Figure S2.

At temperatures below 194 K, the $ClONO_2$ + HCl reaction proceeds extremely efficiently, whereas above 195 K the reaction rate drops so steeply that chlorine enhancement potential is minimal. We see this expected general relationship in Figure 3, where we compare the tropics in November 2009 (Figure 3a) to the southern high latitudes in October 2009 (Figure 3b), when the ozone depletion in Antarctica peaks for the year. Although there is greater scatter in the tropics because some cold regions are isolated from any entrained chlorine, and the enhancement levels in Antarctica reach an order of magnitude higher, we can see that in both cases it is only possible to get enhanced ClO at colder temperatures. Temperature histories can also induce scatter; for example, air at 195 K on one day may contain chlorine activated a day or two earlier when the air was 192 K. A Lagrangian back-trajectory analysis could be used to further

Deleted: 3

Formatted: Subscript

Deleted: 4

evaluate this question, but Figure 3 is sufficient to show that the highest levels of ClO are associated with temperatures below 192 K for both the Antarctic and the tropics.

The coldest temperatures (<192 K) in Figure 2a occur over a broad region of the Western Pacific and are qualitatively consistent with the concept of a stratospheric fountain first described by Newell and Gould-Stewart (1981). Highwood and Hoskins (1998) linked these stratospheric thermal anomalies to the pressure anomalies found in the upper troposphere that form part of the classic response to equatorially-symmetric Matsuno-Gill heating perturbations. This circulation pattern therefore enhances chlorine activation in two ways: by entraining reservoir chlorine in the form of HCl and $ClONO_2$ from higher latitudes (Figures 2b and S2) and by lowering temperatures such that activation proceeds more rapidly (Figure 2a). In addition to the broad region where temperatures are below 192 K, there is a smaller but still substantial region in both hemispheres where they drop below 191 K. This region is roughly symmetric about the equator, but with a greater extent in the northern hemisphere. There are other, smaller regions of extremely cold temperatures to the west and east of the main response pattern which may be associated with convection over land, such as over the Amazon basin.

SD-WACCM's chemistry fields demonstrate the impacts of these cold temperatures and circulation patterns. We focus on two different chemical features at 85 mb for November 2009: enhancement in ClO in Figure 4a and depletion in NO_2 in Figure 4b. As ClO is both a product of the heterogeneous reactions of interest and has very low background levels in the tropics and subtropics, it presents the clearest view of

Deleted: 4

Deleted: 3

Deleted: 5

Deleted: 5

the activation response. Figure S3 compares calculations with heterogeneous chemistry turned on and off to isolate the in-situ chemical enhancement from dynamical transport; the figure shows that heterogeneous chemistry enhances ClO from unperturbed levels of 1 pptv or less in the Tropics in the absence of heterogeneous chemistry to above 25 pptv in the northern hemisphere lobe and above 12 pptv in the southern hemisphere lobe; such high levels of ClO are not normally present equatorward of about ±60° in the months in question. While ClO provides the cleanest signal for chemical activation, NO_2 is a more commonly observable species due to its higher background mixing ratios. Figure 4b shows the expected response in NO_2, of opposite sign to that of ClO, due to the recombination of NO_2 with ClO and subsequent conversion to HNO_3. It is especially illuminating to note how the pattern of chlorine activation curls around with the winds of the anticyclones. In the southern hemisphere in particular, there is a marked decrease in activation near the center of the anticyclone off the northeast coast of Australia. We see continued but decreasing elevated levels in a west-east band across the Pacific. Examination of the reaction rates of the three main heterogeneous chlorine activation reactions described above ($HCl + ClONO_2 \rightarrow Cl_2 + HNO_3$, $H_2O + ClONO_2 \rightarrow HOCl + HNO_3$, and $HCl + HOCl \rightarrow H_2O + Cl_2$) (Figure S4) confirms that the *in-situ* activation is driven by a combination of available chlorine and cold temperatures, with the former limiting activation on the equatorward side and the later limiting it on the poleward side. Both ClO and NO_2 changes span somewhat larger regions than the chemical rates; this is likely associated with advection by the equatorward edges of the subtropical jets or the Kelvin wave part of the Matsuno-Gill wind response. NO_2 changes show a broader pattern than ClO, reflecting the former's longer lifetime in the stratosphere and thus

Deleted: 2

Deleted: 5

Deleted: chemical

Deleted: in question

Deleted: 3

ability to be carried by the circulation. There is more activation in the northern than the southern hemisphere, consistent with the more extensive region of cold temperatures there. It is notable that there is little enhancement of chlorine activation over the equator proper despite the cold temperatures, as the meridional transport of chlorine from higher latitudes weakens dramatically there, in accordance with the Matsuno-Gill meridional wind response vanishing at the equator for symmetric heating.

Although the longitudinally resolved plots give the clearest demonstration of the implications of a Matsuno-Gill type flow for stratospheric chemistry, this activation signal can also be seen in the zonal mean in both ClO and NO_2. Figure 5a and Figure 5b show the ClO and NO_2 mixing ratios for November 2009 at 85 mb for the Chem-Dyn-Vol run and the NoHet40NS run. A partial zonal mean from 100°E to 250°E emphasizes the region of interest while excluding the influence of the continental landmasses, but the same features are present in the full zonal mean (Figure S5) despite dilution from chemically quiescent longitudes. ClO shows an extremely clear dual hemisphere enhancement, stronger in the northern hemisphere, with background levels nearly zero in the absence of heterogeneous chemistry. NO_2 has a more pronounced hemispheric asymmetry, although the signal is present in both. The feature in NO_2 near 10°N is especially significant, as the Chem-Dyn-Vol mixing ratio of ~60 pptv, compared to the NoHet40NS concentration of ~200 pptv, should be observable. Perturbations are even larger at some longitudes as shown in Figure 4.

Deleted: 6

Deleted: 6

Deleted: 4

Deleted: 5

4 Discussion

We find clear signals of enhancement in ClO and depletion in NO_2 in SD-WACCM in the tropical lower stratosphere in months near the equinoxes due to the presence of heterogeneous chemistry on liquid sulfuric acid aerosols. We present results from November 2009 and find similar patterns in several other months as well, as shown in the ClO differences over the entire time series (Figure S6). In particular, November 2011 (Figure S6d), December 2011 (Figure S6a), April 2009 (Figure S6b), and April 2011 (Figure S6b) show double bullseyes. Boreal summer (Figure S6c) and austral summer (Figure S6a) are both dominated by single-hemisphere enhancements associated with their monsoons. The strong East Asian Summer Monsoon anticyclone leads to the largest chlorine enhancement of these asymmetric heating responses, confirming what was previously found in Solomon et al., 2016. It is worth noting that, while November 2010-January 2011 have very high enhancement, the Merapi volcano erupted at the end of October 2010, increasing the aerosol surface areas and heterogeneous reaction rates, and likely dominates the signal for months.

We have systematically traced the chlorine activation back to the effects of a Matsuno-Gill circulation pattern caused by diabatic heating in equatorial regions of the Western Pacific. This circulation pattern includes anticyclones in the lower stratosphere of both hemispheres that entrain chlorine to lower latitudes, as well as very cold lower-stratospheric temperatures overlying regions where the tropopause is high. Winds and temperatures combine to drive efficient heterogeneous chlorine activation. The changes in ClO and NO_2 background mixing ratios provide a testable signature of this mechanism that should be visible to future measurement campaigns in the region,

Deleted: 5
Deleted: 5
Deleted: 5
Deleted: 5
Deleted: 5
Deleted: this
Deleted: enhancement

particularly using airborne instruments. Unfortunately, the current generation of chemistry-focused satellites does not measure ClO in the tropical UTLS, but should that change this pattern should also be visible on a large scale as seen in the model. While the differences between the SD-WACCM runs we present successfully isolate the signal of chlorine activation due to heterogenous reactions, the underlying meteorological fields and thus the Matsuno-Gill circulations are the same for all runs. To quantify the importance of these for transporting chlorine, runs with modified dynamics that suppress the Matsuno-Gill response would be required. While such comparisons are beyond the scope of this study, they could be a useful component of future ones.

Although the years we look at in this study were devoid of major volcanic eruptions, in the past decade numerous studies have shown that aerosols from the more frequent, moderate-sized volcanoes have a discernible impact on many aspects of stratospheric chemistry (Solomon et al. 2011, Naik et al. 2017, Adams et al. 2017, Wilka et al. 2018). Sarychev Peak erupted in June 2009 and lofted measurable sulfur to the stratosphere, so November 2009 was not “volcanically clean.” Nor was 2011, due to the Nabro eruption in June of that year. However, as volcanically clean years seem to be more the exception than the rule (Mills et al. 2016, Vernier et al. 2011), at least in recent decades, 2009 may be a fairly typical year in terms of tropical sulfate levels.

The model chemistry relies on several assumptions about heterogeneous chemistry whose validity could impact our results. The parameterized heterogeneous activation rates are based on laboratory studies that contain few direct measurements

at the coldest temperatures, and have not been updated for almost two decades. Furthermore, these studies assumed pure liquid H_2O/H_2SO_4 mixtures, so that the effects of freezing and of any doping with pollutant nitrates or organics are poorly constrained. The extent to which these matter in the real world depends on both the aerosol composition of the tropical lower stratosphere and the degree to which sulfates are internally versus externally mixed with other species. The degree of accuracy with which models capture relevant stratospheric aerosol processes and composition changes is an area of active research (Kremser et al. 2016 and references therein). One recent study (Höpfner et al. 2019) found elevated levels of solid ammonium nitrate in the upper troposphere during the Asian summer monsoon due to convective uplift of NH_3. However, they did not find elevated ammonium nitrate outside of the summer monsoon months, i.e., for the months of interest here. Further, sulfate aerosols can be expected to be dominant in volcanically perturbed periods.

While the version of SD-WACCM we use does not account for heterogeneous chemistry on cirrus ice cloud particles, we expect such reactions to enhance our modeled activation. Cirrus chemistry parameterizations are subject to large uncertainties, but we test our expectation by running SD-WACCM with an ice chemistry parameterization implemented for the four years of interest and plot the ClO mixing ratios in Figure 6, along with the Chem-Dyn-Vol and NoHet40NS runs for the same Pacific region of interest as Figure 5. We see in Figure 6 that ice chemistry increases activation, as expected, but the magnitude of its impact varies greatly both among years and between hemispheres. For November 2009, ice chemistry appears to enhance ClO

Deleted: 7

Deleted: 6

Deleted: 7

more in the Southern Hemisphere (Figure 6b) than the Northern Hemisphere (Figure 6a), but in November 2010 there is little effect in either hemisphere. The relative importance of cirrus clouds is an ongoing area of study, but it is important to note that the enhancements seen in Figure 6, regardless of season, occur in addition to activation caused by liquid sulfuric acid aerosols, and we do not see any significant enhancements in the absence of liquid sulfuric acid aerosol-driven activation. Thus, we feel confident that our results capture the main features of chlorine activation in the tropical UTLS, even without considering cirrus input.

Deleted: 7

An additional source of uncertainty in the model results comes from the adopted temperature profiles. MERRA temperatures near the tropopause, to which SD-WACCM is relaxed, assimilate both satellite and in-situ observations, so we expect that they capture the mean structure well. However, the number of levels in the UTLS is relatively small, and may fail to capture some of the variance in temperature structure often seen in higher vertical resolution radiosondes, especially due to situations such as a double-peaked cold point tropopause or small-scale wave activity. We recognize that this smoothing of the temperature structure will mute some of the corresponding vertical structure in the chemistry, and in particular may underestimate activation if the cold point occurs between model levels. This is an active area for further research and the importance of temperature resolution for chemistry could inform considerations of future sub-grid scale modelling parameterizations, as well as be a target of investigation for higher-resolution models.

Another promising direction for further exploration is the role that wave activity on different timescales has on the likelihood and lifetime of the patterns that we investigate here. Tropical winds, temperatures, and resultant chemistry patterns are influenced from year-to-year by El Niño-Southern Oscillation and the Quasi-Biennial Oscillation, and on sub-seasonal timescales by the Madden-Julien Oscillation and mixing from midlatitude eddies. As we have examined only a monthly-mean response, we recognize that on shorter time scales the activation could be both stronger and more localized. This is especially likely in the case of modulation of convection by the MJO, which varies in location over its cycle and in strength between different events. While it is intriguing that 2009 and 2011 both seem to display more activation in fall and spring (Figure S6), the current study does not span enough years to determine what dynamical phases or combinations thereof are most responsible for influencing chemistry. A systematic investigation of a longer time series could also help quantify the influence of summer monsoonal circulations of varying strength on this chemistry. Quantifying how both the background state of the atmosphere and the activity of more transient phenomena influence the likelihood of finding these patterns is an area of ongoing investigation.

Deleted: 5

Deleted:

5 Conclusions

This study has expanded our knowledge of where heterogeneous chlorine activation chemistry can take place in months near the equinoxes, and revealed new connections between tropical meteorology and stratospheric chemistry. The ClO and NO_2 levels we have modeled provide observable targets for future aircraft campaigns or

satellites focused on the tropical UTLS. For example, measurements of the anomalies seen in both hemispheres (as in Figure 4) would serve as a characteristic signature of the response as described here. Such campaigns could also use this chemistry to deepen our understanding of the stratospheric equatorially-symmetric Matsuno-Gill circulation and transport patterns, with chemical enhancements providing observable indicators for dynamical studies.

Deleted: 5

Furthermore, while we have focused on the heterogeneous chlorine reactions most relevant for ozone depletion in this region, it is notable that other chemical constituents and processes will also be affected. For example, all reactants with a steep equator-to-pole concentration gradient are expected to be affected by the Matsuno-Gill wind pattern described here. Reactions with a sufficiently strong temperature sensitivity will also be influenced. For both chlorine-dependent and other reactions, continuing to investigate the impacts of zonally asymmetric circulation patterns on atmospheric chemistry is an area ripe for further research.

Data Availability Statement

We thank NOAA's Earth System Research Laboratory for the GCPC rainfall data (available freely online at esrl.noaa.gov/psd/data/gridded/data.gcpc.html). We thank NASA Goddard Space Flight Center for the MERRA data (available freely online at http://disc.sci.gsfc.nasa.gov/). WACCM is a component of the Community Earth System

Model (CESM), which is supported by the National Science Foundation. WACCM runs are available at https://acomstaff.acom.ucar.edu/dkin/JAS_Wilka_2020/.

Acknowledgements

We would like to acknowledge high-performance computing support from Cheyenne (doi:10.5065/D6RX99HX) provided by NCAR's Computational and Information Systems Laboratory, sponsored by the National Science Foundation. CW, SS, and TC are grateful for partial support under NSF grant 1906719 from the atmospheric chemistry division. DK is grateful for partial support under NASA ACMAP grant 80NSSC19K0952.

459 **References Cited**

460

461 Adames, Á. F., & Wallace, J. M., 2017: On the tropical atmospheric signature of El Niño,
462 *Journal of the Atmospheric Sciences*, **74(6)**, 1923-1939.

463

464 Adams, C., Bourassa, A. E., McLinden, C. A., Sioris, C. E., Clarmann, T. V., Funke, B.,
465 ... & Degenstein, D. A., 2017: Effect of volcanic aerosol on stratospheric NO 2
466 and N 2 O 5 from 2002–2014 as measured by Odin-OSIRIS and Envisat-MIPAS,
467 *Atmospheric Chemistry and Physics*, **17(13)**, 8063-8080.

468

469 Adler, R. F., Huffman, G. J., Chang, A., Ferraro, R., Xie, P. P., Janowiak, J., ... &
470 Gruber, A., 2003: The version-2 global precipitation climatology project (GPCP)
471 monthly precipitation analysis (1979–present), *Journal of hydrometeorology*, **4(6)**,
472 1147-1167.

473

474 Anderson, J. G., Weisenstein, D. K., Bowman, K. P., Homeyer, C. R., Smith, J. B.,
475 Wilmouth, D. M., ... & Wofsy, S. C., 2017: Stratospheric ozone over the United
476 States in summer linked to observations of convection and temperature via
477 chlorine and bromine catalysis, *Proceedings of the National Academy of*
478 *Sciences*, **114(25)**, E4905-E4913.

479

480 Froidevaux, L., Kinnison, D. E., Wang, R., Anderson, J., & Fuller, R. A., 2019:
481 Evaluation of CESM1 (WACCM) free-running and specified dynamics

atmospheric composition simulations using global multispecies satellite data records, *Atmospheric Chemistry and Physics*, **19(7)**, 4783-4821.

Gill, A. E., 1980: Some simple solutions for heat-induced tropical circulation. *Quarterly Journal of the Royal Meteorological Society*, **106(449)**, 447-462.

Highwood, E. J., & Hoskins, B. J., 1998: The tropical tropopause. *Quarterly Journal of the Royal Meteorological Society*, **124(549)**, 1579-1604.

Höpfner, M., Ungermann, J., Borrmann, S., Wagner, R., Spang, R., Riese, M., ... & Cairo, F., 2019: Ammonium nitrate particles formed in upper troposphere from ground ammonia sources during Asian monsoons, *Nature Geoscience*, **12**, 608-612.

Jin, F., & Hoskins, B. J., 1995: The direct response to tropical heating in a baroclinic atmosphere, *Journal of the Atmospheric Sciences*, **52(3)**, 307-319.

Kremser, S., Thomason, L. W., von Hobe, M., Hermann, M., Deshler, T., Timmreck, C., ... & Fueglistaler, S., 2016: Stratospheric aerosol—Observations, processes, and impact on climate, *Reviews of Geophysics*, **54(2)**, 278-335.

503 Marsh, D. R., Mills, M. J., Kinnison, D. E., Lamarque, J. F., Calvo, N., & Polvani, L. M.,
504 2013: Climate change from 1850 to 2005 simulated in CESM1 (WACCM),
505 *Journal of Climate*, **26(19)**, 7372-7391.
506
507 Matsuno, T., 1966: Quasi-geostrophic motions in the equatorial area, *Journal of the*
508 *Meteorological Society of Japan. Ser. II*, **44(1)**, 25-43.
509
510 Mills, M. J., Richter, J. H., Tilmes, S., Kravitz, B., MacMartin, D. G., Glanville, A. A., ... &
511 Gettelman, A., 2017: Radiative and chemical response to interactive
512 stratospheric sulfate aerosols in fully coupled CESM1 (WACCM), *Journal of*
513 *Geophysical Research: Atmospheres*, **122(23)**, 13-061.
514
Mills, M. J., Schmidt, A., Easter, R., Solomon, S., Kinnison, D. E., Ghan, S. J., ... &
Gettelman, A., 2016: Global volcanic aerosol properties derived from emissions,
1990–2014, using CESM1 (WACCM), *Journal of Geophysical Research:*
Atmospheres, **121(5)**, 2332-2348.

Naik, V., Horowitz, L. W., Daniel Schwarzkopf, M., & Lin, M., 2017: Impact of volcanic
aerosols on stratospheric ozone recovery, *Journal of Geophysical Research:*
Atmospheres, **122(17)**, 9515-9528.

Neely, R., & Schmidt, A., 2016: VolcanEESM: Global volcanic sulphur dioxide (SO2) emissions database from 1850 to present–Version 1.0, *Cent. Environ. Data Anal., doi.org/10.5285/76ebdc0b-0eed-4f70-b89e-55e606bcd568*

Newell, R. E., & Gould-Stewart, S., 1981: A stratospheric fountain? *Journal of the Atmospheric Sciences*, **38(12)**, 2789-2796.

Rienecker, M. M., Suarez, M. J., Gelaro, R., Todling, R., Bacmeister, J., Liu, E., ... & Bloom, S., 2011: MERRA: NASA's modern-era retrospective analysis for research and applications, *Journal of Climate*, **24(14)**, 3624-3648.

Robrecht, S., Vogel, B., Grooß, J. U., Rosenlof, K., Thornberry, T., Rollins, A., ... & Müller, R., 2019: Mechanism of ozone loss under enhanced water vapour conditions in the mid-latitude lower stratosphere in summer, *Atmospheric Chemistry and Physics*, **19(9)**, 5805-5833.

Rodwell, M. J., & Hoskins, B. J., 2001: Subtropical anticyclones and summer monsoons, *Journal of Climate*, **14(15)**, 3192-3211.

Shi, Q., Jayne, J. T., Kolb, C. E., Worsnop, D. R., & Davidovits, P., 2001: Kinetic model for reaction of ClONO2 with H2O and HCl and HOCl with HCl in sulfuric acid solutions, *Journal of Geophysical Research: Atmospheres*, **106(D20)**, 24259-24274.

Solomon, S., Garcia, R. R., Rowland, F. S., & Wuebbles, D. J., 1986: On the depletion of Antarctic ozone, *Nature*, **321(6072)**, 755.

Solomon, S., 1999: Stratospheric ozone depletion: A review of concepts and history, *Reviews of Geophysics*, **37(3)**, 275-316.

Solomon, S., Daniel, J. S., Neely, R. R., Vernier, J. P., Dutton, E. G., & Thomason, L. W., 2011: The persistently variable "background" stratospheric aerosol layer and global climate change, *Science*, **333(6044)**, 866-870.

Solomon, S., Kinnison, D., Garcia, R. R., Bandoro, J., Mills, M., Wilka, C., ... & Höpfner, M., 2016: Monsoon circulations and tropical heterogeneous chlorine chemistry in the stratosphere, *Geophysical Research Letters*, **43(24)**, 12-624.

Vernier, J. P., Thomason, L. W., Pommereau, J. P., Bourassa, A., Pelon, J., Garnier, A., ... & Vargas, F., 2011: Major influence of tropical volcanic eruptions on the stratospheric aerosol layer during the last decade, *Geophysical Research Letters*, **38(12)**.

Wilka, C., Shah, K., Stone, K., Solomon, S., Kinnison, D., Mills, M., ... & Neely III, R. R., 2018: On the role of heterogeneous chemistry in ozone depletion and recovery, *Geophysical Research Letters*, **45(15)**, 7835-7842.

561

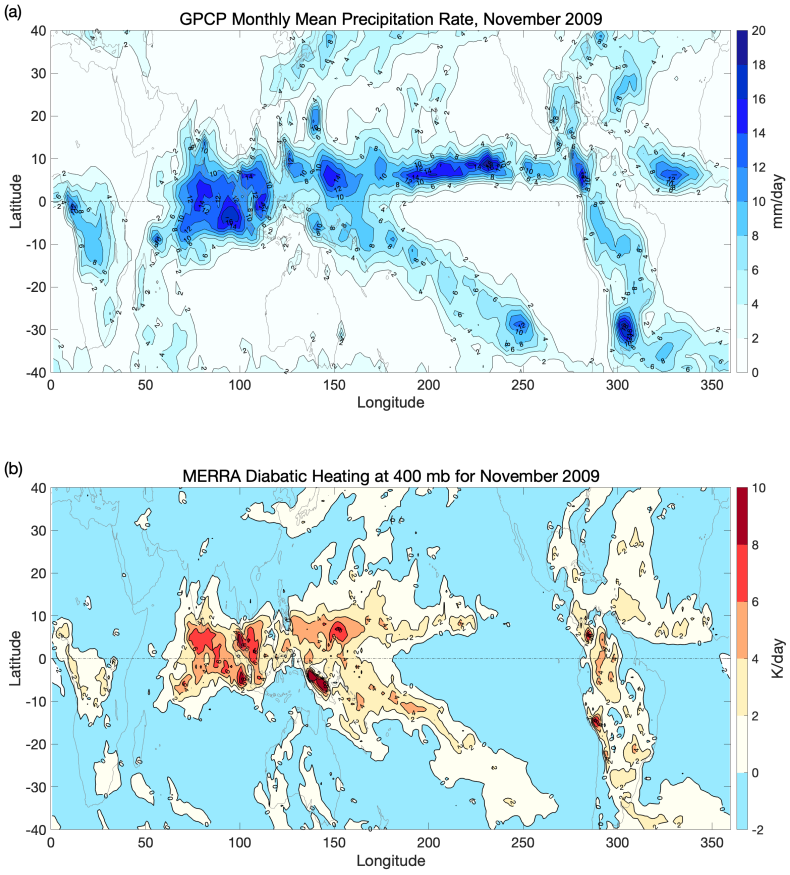

562

563

564 **Figure 1. a)** Precipitation (mm/day) from the GPCP and **b)** diabatic heating rates

565 (K/day) at 400 mb from MERRA reanalysis from 40°N to 40°S, averaged for November

566 2009.

567

568

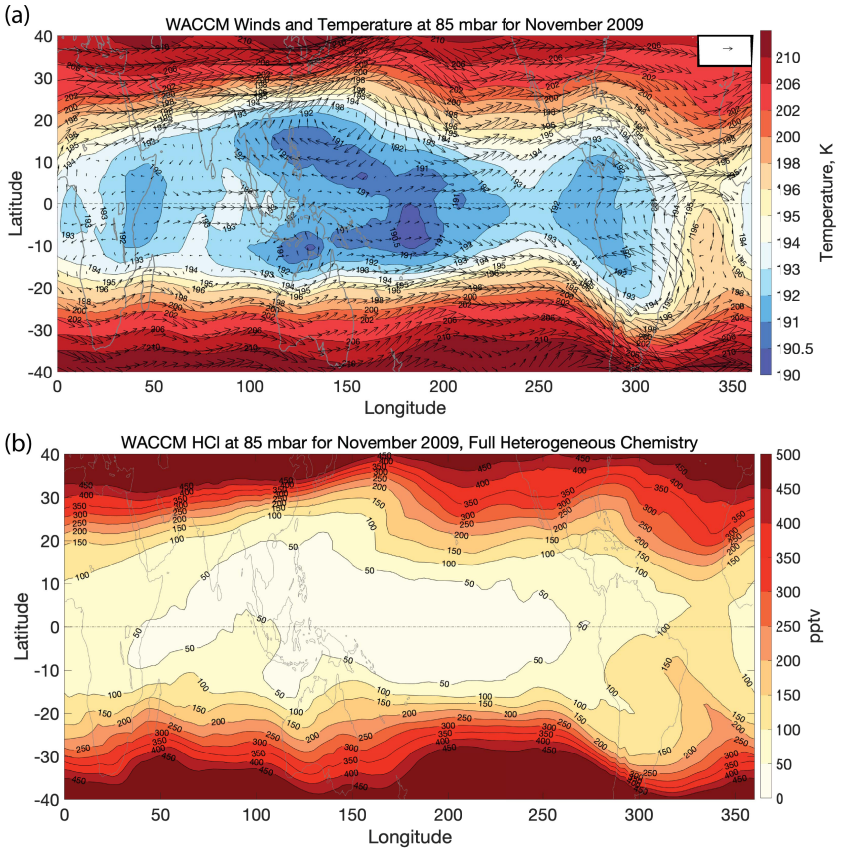

Figure 2. **a)** Monthly mean WACCM horizontal flow and temperature (K) at 85 mb from 40°N to 40°S for November 2009. The winds are shown as vectors, with the length of the tail corresponding to the strength of the wind. A 5 m/s vector is displayed in the upper right for scale. **b)** Monthly mean WACCM HCl volume mixing ratios at 85 mbar in the tropics for November 2009. Heterogeneous chemistry is turned on at all latitudes.

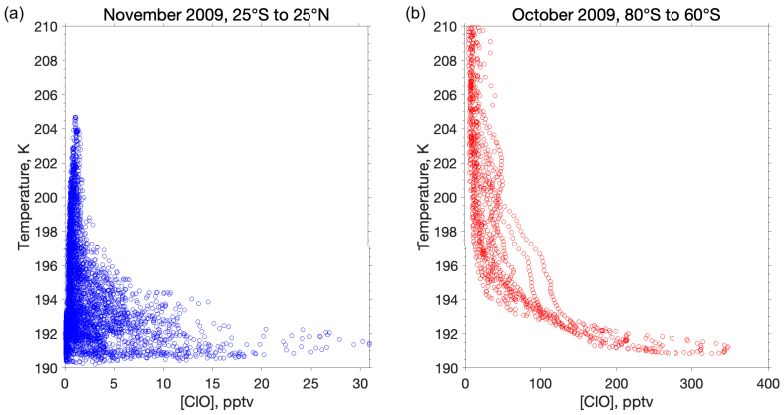

Figure 3. Distribution of ClO mixing ratios and associated temperatures in **(a)** the tropics for November 2009 and in **(b)** the Antarctic for October 2009. Both plots are at 85 mbar for all longitudes.

582

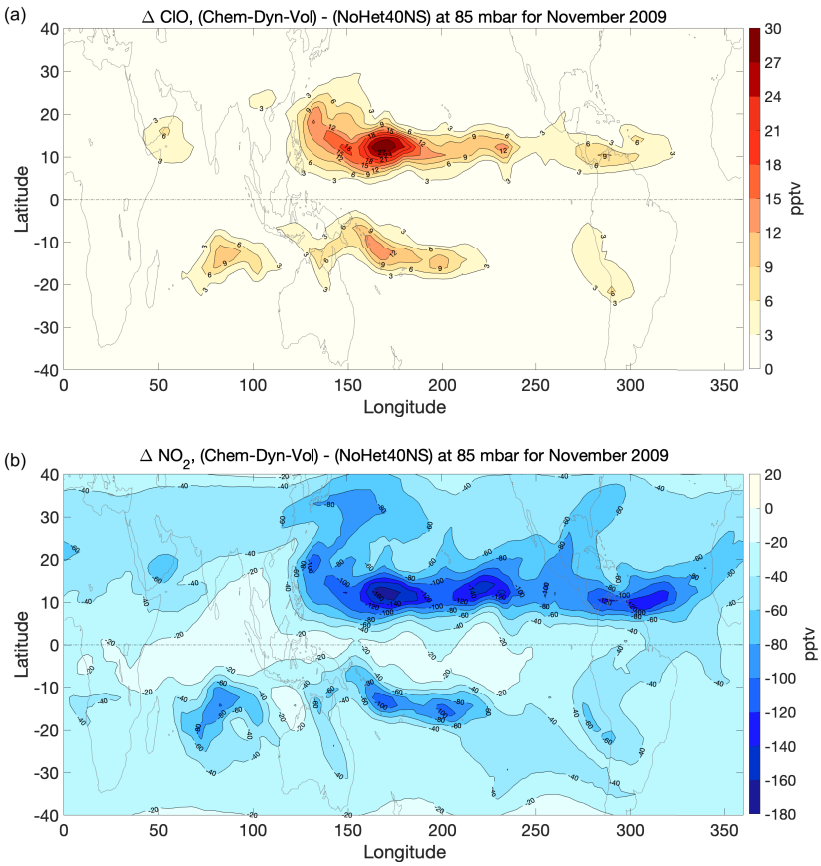

583

584

585 **Figure 4**. Differences in the monthly mean distribution of **(a)** ClO and **(b)** NO_2 at 85 mb
586 in SD-WACCM between the runs with and without heterogeneous chlorine and bromine
587 chemistry turned on in the tropics. Red values show relative enhancement and blue
588 indicates relative depletion.

589

590

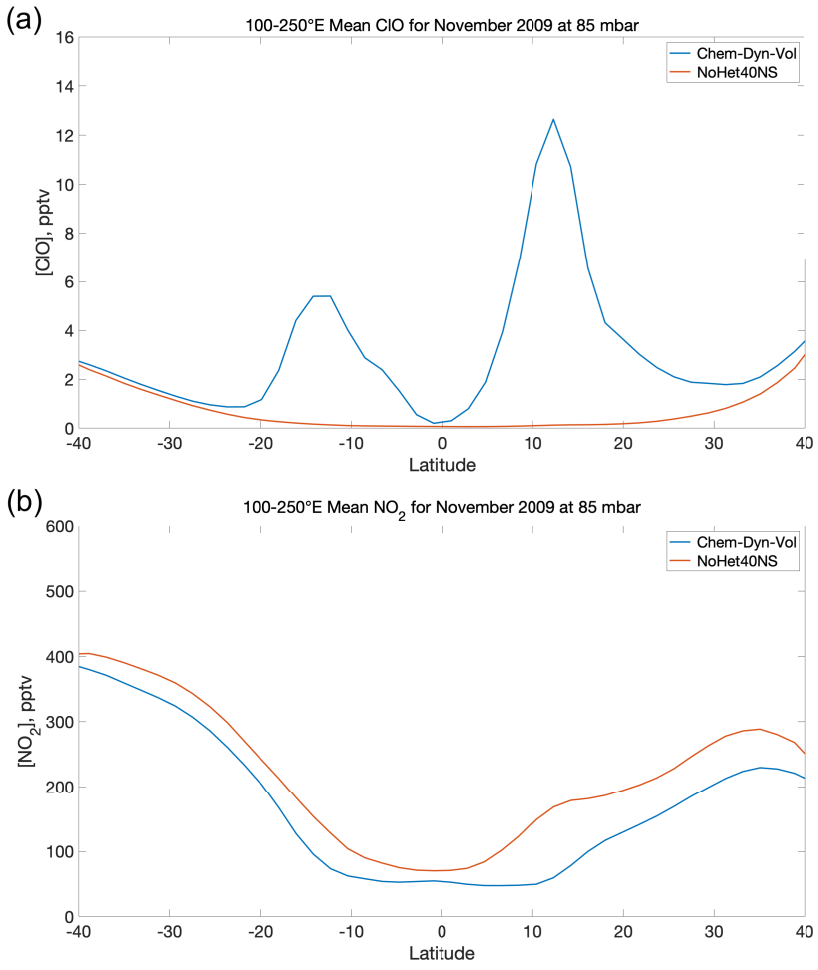

591

592 **Figure 5.** Monthly longitudinal means from 100° to 250°E for **(a)** ClO and **(b)** NO_2 in SD-
593 WACCM at 85 mb from 40°S to 40°N for November 2009. The blue line is the Chem-
594 Dyn-Vol run with full heterogeneous chemistry turned on and the red line is the
595 NoHet40NS run with heterogeneous chlorine and bromine chemistry turned off in the
596 tropics.

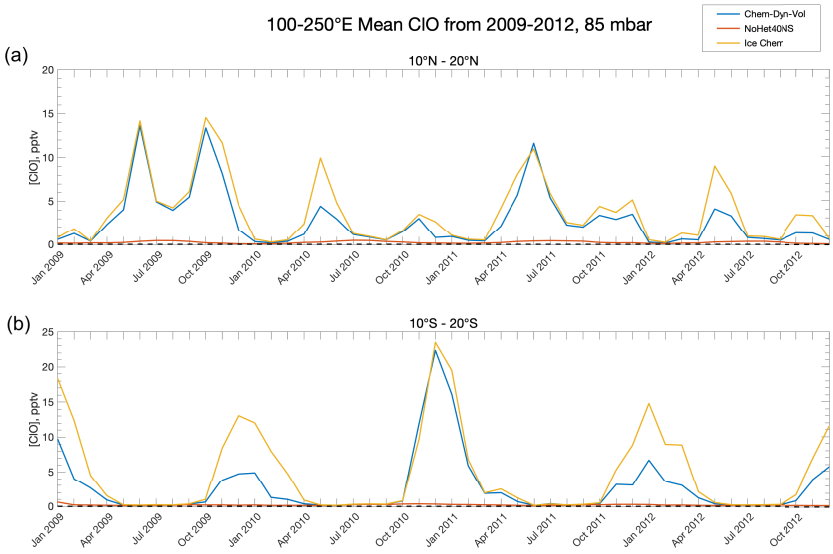

Figure 6. Time series of monthly mean ClO over the Pacific in the **(a)** Northern Hemisphere and **(b)** Southern Hemisphere tropics. Latitude bands are chosen to maximize the activation signal and isolate inter-hemispheric differences. The blue line is the Chem-Dyn-Vol run with full heterogeneous chemistry turned on but no ice chemistry, the red line is the NoHet40NS run with heterogeneous chlorine and bromine chemistry turned off in the tropics, and the yellow line is the Ice Chem run with full heterogeneous chemistry and an additional ice chemistry parameterization included.